

sible for giving Ho a stronger tendency toward a spiral magnetic order do not result in a measurably

larger Kohn-type anomaly in the phonon spectrum of Ho.

†Research sponsored by the U.S. Atomic Energy Commission under contract with the Union Carbide Corporation.

*Present address: Bhabha Atomic Energy Research Centre, Trombay, Bombay, India.

¹J. C. Gylden Houmann and R. M. Nicklow, *Phys. Rev. B* **1**, 3943 (1970).

²J. A. Leake, V. J. Minkiewicz, and G. Shirane, *Solid State Commun.* **7**, 535 (1969).

³B. C. Gerstein, M. Griffel, L. D. Jennings, R. E. Miller, R. E. Skochdopole, and F. H. Spedding, *J. Chem. Phys.* **27**, 394 (1957).

⁴L. J. Raubenheimer and G. Gilat, *Phys. Rev.* **157**, 586 (1967).

⁵R. J. Pollina and B. Luthi, *Phys. Rev.* **177**, 841 (1969).

⁶S. B. Palmer, *J. Phys. Chem. Solids* **31**, 143 (1970).

⁷O. V. Lounasmaa and L. J. Sundström, *Phys. Rev.* **150**, 399 (1966); **158**, 591 (1967).

⁸R. J. Elliott and F. A. Wedgwood, *Proc. Soc. (London)* **81**, 846 (1963).

⁹W. E. Evenson and S. H. Liu, *Phys. Rev.* **178**, 783 (1969).

¹⁰B. C. Gerstein, W. A. Taylor, W. D. Shickell, and F. H. Spedding, *Phys. Rev.* **51**, 2924 (1969).

¹¹H. V. Culbert, *Phys. Rev.* **156**, 701 (1967).

¹²M. Rosen, *Phys. Rev. Letters* **19**, 695 (1967).

PHYSICAL REVIEW B

VOLUME 3, NUMBER 4

15 FEBRUARY 1971

Study of the Martensitic Phase Transition in Sodium†

Galen K. Straub* and Duane C. Wallace

Sandia Laboratories, Albuquerque, New Mexico 87115

(Received 9 July 1970)

The martensitic transformation in sodium is studied by means of a local pseudopotential theory. The total Helmholtz free energy is calculated as a function of temperature and crystal configuration for both the bcc and hcp phases of sodium. At $T=0$, the hcp phase is found to be stable, while the bcc phase is found to be stable at high temperatures. The inclusion of the zero-point energy at $T=0$ gives improved agreement with the experimentally determined energy differences between the bcc and hcp phases. It is found that the thermal expansion of the crystal does not play a significant role in the phase transition and the transition from hcp to bcc as the temperature increases can be explained by thermodynamic arguments.

I. INTRODUCTION

A martensitic phase transition has been observed in sodium around 36 °K.¹ As the temperature is lowered, the high-temperature bcc structure changes to a close-packed hexagonal structure (non-ideal ratio). In order to study this transition, we have used a simple local pseudopotential model to calculate the Helmholtz free energy for both the bcc and hcp structures. Previous calculations^{2,3} to determine the stable crystal structure of sodium have calculated the band structure and electrostatic energies at $T=0$ of the bcc and hcp phases at fixed volume. In the present calculation, the total free energy as a function of the crystal configuration is calculated and then minimized at each temperature with respect to the configuration. Our calculations show an energy difference at $T=0$ that is approximately twice the experimentally determined energy difference, and the total free energy predicts a phase transition from the cubic to hexagonal structure at a transition temperature about seven times the observed transition temperature.

In Sec. II the local pseudopotential used in this calculation is briefly described, and in Sec. III the calculation of the total free energy is described with emphasis on the hexagonal free energy and the procedure used to minimize it. In Sec. IV we discuss the relative importance of volume-dependent vs structural-dependent terms in the free energy, and give thermodynamic arguments for the explanation of the cubic to hexagonal transition.

II. DESCRIPTION OF LOCAL PSEUDOPOTENTIAL

One of the features of pseudopotential theory is that the pseudopotential can be separated into terms that are structure dependent and terms that are dependent only upon the total crystal volume. Thus, one is able to compare different crystal structures and, as in this case, specifically incorporate the structural differences in the calculation of the total Helmholtz free energy.

Because of its analytical simplicity, we have chosen Harrison's modified point-ion pseudopotential and included a Born-Mayer repulsion between ion cores. The pseudopotential contains two ad-

justable parameters and the Born-Mayer repulsion contains one parameter. The three parameters were determined by fitting the relevant experimental data, corrected to $T = 0^\circ\text{K}$ and zero pressure, to the appropriate derivatives of the static lattice potential, neglecting the zero-point vibrational energy.⁴ A fit to the corrected experimental data for the binding energy per atom of the metal, ionization energy per ion, the bulk modulus, and the requirement that the pressure be zero, gave correlated values of the parameters with a small degree of arbitrariness. This arbitrariness was removed by requiring agreement between calculated and measured values of the average of the phonon frequencies squared. The fitting procedure was used for only the bcc phase of sodium. Since the lattice-potential parameters are independent of structure and volume, the same parameters as determined by the bcc data were used in the calculation of quantities for the hcp phase, and no additional fitting to hcp data was done.

The total potential is the sum of the Born-Mayer repulsion between ion cores (U_R), the electrostatic energy of the lattice of point ions of charge $+Ze$ in a uniform compensating background (U_{ES}), the uniform electron-gas energy (U_{EG}), and the band-structure energy (U_{BS}). The calculation of the electrostatic energy for the hcp structure is more difficult than for the bcc structure. The electrostatic energy may be written⁴

$$U_{ES} = N \left(\frac{Z^2 e^2}{2} \right) \left(\frac{4\pi}{\Omega_a} \sum_{\vec{q}} S_{\vec{q}} S_{-\vec{q}} q^{-2} e^{-q^2/4\pi^2} + N^{-1} \sum_{nn'} \frac{\text{erfc}(\eta |\vec{r}_n - \vec{r}_{n'}|)}{|\vec{r}_n - \vec{r}_{n'}|} - [(2\eta/\sqrt{\pi}) + (\pi/\eta^2 \Omega_a)] \right), \quad (1)$$

where the structure factor is given by

$$S_{\vec{q}} = N^{-1} \sum_n e^{-i\vec{q} \cdot \vec{r}_n}. \quad (2)$$

N is the number of atoms in the crystal and the volume per atom is given by $\Omega_a = \Omega N^{-1}$. The Ewald convergence factor η (which is arbitrary) was chosen so that the contributions from the first two terms in U_{ES} (the wave number sum and double-lattice sum) were of the same order of magnitude. The electrostatic energy may be written^{5(a)}

$$U_{ES} = -N\alpha Z^{5/3}/r_s, \quad (3)$$

where

$$\Omega_a = \frac{1}{3} 4\pi r_s^3 \quad (4)$$

defines r_s and for the bcc lattice

$$\alpha_{\text{bcc}} = +1.79186. \quad (5)$$

α_{bcc} is independent of the cube size, while for the hcp lattice, α_{hcp} depends upon the c/a ratio. We chose to calculate the electrostatic energy from Eq. (1) for both bcc and hcp structures. For all the volumes calculated, α_{bcc} agreed with Eq. (5). α_{hcp} is a maximum near the ideal c/a ratio and

$$\alpha_{\text{hcp}} = +1.79168, \quad c/a = \sqrt{\frac{8}{3}}. \quad (6)$$

α_{hcp} agrees with Harrison's values² for both ideal and nonideal ratios of c/a .^{5(b)}

Care must also be exercised in the calculation of the band-structure energy for the hexagonal lattice where

$$S_{\vec{q}} = \frac{1}{2} \delta_{\vec{q}\vec{Q}} [1 + e^{-i\vec{q} \cdot \vec{\delta}}]. \quad (7)$$

The basis vectors for the hexagonal lattice are chosen such that one atom per unit cell lies on each lattice point and the second atom per unit cell is located at $\vec{\delta}$ with respect to each lattice point. The \vec{Q} are the reciprocal-lattice vectors. The band-structure energy is then given by

$$U_{BS} = \frac{1}{2} N \sum_{\vec{Q}} F_{\vec{Q}} [1 + \cos(\vec{Q} \cdot \vec{\delta})], \quad (8)$$

where $F_{\vec{Q}}$ is the energy-wave-number characteristic. The electron-gas energy and the overlap repulsion energy are easily calculated, as described in Ref. 4.

III. CALCULATION OF TOTAL FREE ENERGY

The calculation of the total free energy systematically divides into the calculation of the static potential energy, the lattice-dynamical calculation for the determination of the phonon frequencies, the calculation of the free-electron gas contribution to the free energy, and finally the minimization of the total free energy as dependent upon temperature and crystal configuration.

The total free energy may be written

$$F(T, V) = U_{\text{static}} + \frac{1}{2} \sum_{\vec{k}s} \hbar \omega_{\vec{k}s} + k_B T \sum_{\vec{k}s} \ln(1 - e^{-\beta \hbar \omega_{\vec{k}s}}) - \frac{1}{2} \Gamma T^2, \quad (9)$$

where the first term on the right-hand side is the energy of the static crystal, the second term is the zero-point energy of the lattice vibrations, and the third term is the phonon contribution to the temperature-dependent free energy. The last term is the electron-gas contribution to the free energy, which we calculate in the free-electron approximation, where

$$\Gamma = N\pi^2 k_B^2 / 2\epsilon_F. \quad (10)$$

k_B is the Boltzmann constant and ϵ_F is the free-electron-gas Fermi energy. This term is dependent only on the volume per electron and is independent of the crystal structure.

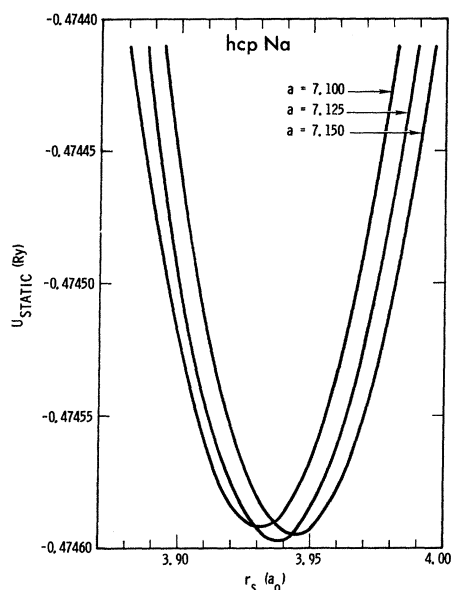


FIG. 1. hcp static potential energy for different values of a .

The static potential for the bcc structure can be calculated as a function of the cube edge, or equivalently as a function of r_s . For the hcp structure, the static potential is a function of both c and a and we chose to write the volume dependence of the potential as a function of a and r_s , where

$$r_s^3 = (\sqrt{27}/16\pi) a^2 c \quad (11)$$

This choice of parameters to describe the lattice structure promotes an easier comparison of bcc and hcp potentials, since they can be compared at the same r_s .

Figure 1 shows the hcp static potential energy plotted as a function of r_s , where each of the three curves is for a different value of a . These curves show the sensitivity of the potential to the rearrangement of the atoms when the volume (r_s) is kept fixed. Thus, one can easily obtain the minimum value of the potential at each r_s as a function of the crystal configuration.

Figure 2 shows a comparison of the $T=0$ free energy for both the hcp and bcc structures with the points of the hcp curve obtained by first minimizing the free energy with respect to the crystal configuration at each volume (r_s), and then plotting only the minimum values of the free energy. The hcp and bcc potentials have their minima at about the same volume and their energy difference is on the order of the transition temperature for the bcc to hcp transition. Table I gives the comparison of the bcc and hcp lattice parameters with experiment. The lattice parameters given were determined by minimizing the static potential and free energy at

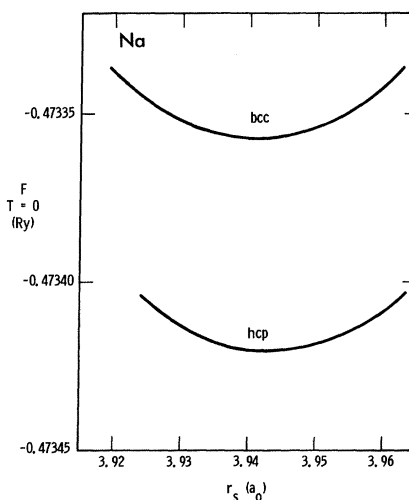


FIG. 2. $T=0$ free energy for hcp and bcc crystal structures of sodium excluding the zero-point contribution.

$T=0$ with respect to the crystal configuration.

From the expression for U_{ES} , U_{BS} , and the Born-Mayer repulsion potential, we may calculate the harmonic potential-energy coefficients and construct the dynamical matrices $\tilde{a}_{\vec{k}}$ for all phonon wave vectors \vec{k} in the first Brillouin zone. For the bcc structure, the $\tilde{a}_{\vec{k}}$ are real symmetric 3×3 matrices with eigenvalues $M(\omega_{\vec{k}s})^2$ and phonon polarization vectors $\vec{v}_{\vec{k}s}$, $s=1,2,3$, where M is the mass of the ions, and $\omega_{\vec{k}s}$ are the phonon circular frequencies. The calculation proceeds as in Ref. 4, but now we must perform the calculation for each crystal configuration of interest. The phonon frequencies and polarization vectors were calculated for 284 points in $\frac{1}{48}$ of the first Brillouin zone.

For the hcp structure, $a_{\vec{k}}$ is a 6×6 Hermitian matrix, and by the proper similarity transformation it can be written in the form

$$a_{\vec{k}} = \begin{pmatrix} \frac{u+v_1}{v_0} & \frac{v_0}{u-v_1} \end{pmatrix}, \quad (12)$$

TABLE I. Comparison of calculated hcp and bcc lattice parameters with experiment. Column A was determined from the static potential only, while column B includes the zero-point energy. The experimental values of Barrett (Ref. 1) are given in column C. Units are Bohr radii (a_0).

Lattice parameter	A	B	C
bcc: r_s	3.939	3.954	3.941
hcp: r_s	3.940	3.950	3.935
a	7.125	7.150	7.119
c	11.636	11.662	11.630

where \vec{u} , \vec{v}_0 , \vec{v}_1 are real symmetric 3×3 matrices labeled by the Cartesian indices ii' :

$$\begin{aligned} u_{ii'} = & \sum_{\vec{q}} G_{|\vec{k}+\vec{q}|} (\vec{k}+\vec{q})_i (\vec{k}+\vec{q})_{i'} \\ & - \delta_{ii'} \sum_{\vec{q}} G_{|\vec{q}|} [1 + \cos(\vec{Q} \cdot \vec{\delta})] \\ & + \sum_n' A_{ii'}(\vec{r}_n) [\cos(\vec{k} \cdot \vec{r}_n) - \delta_{ii'}] \\ & - \delta_{ii'} \sum_n A_{ii'}(\vec{r}_n + \vec{\delta}), \end{aligned} \quad (13)$$

where \sum' means to exclude the \vec{Q} (or \vec{r}_n) equal zero term. $A_{ii'}(\vec{r}_n)$ is the total potential-energy coefficient for the lattice sums and is composed of the lattice-sum contributions to the electrostatic energy plus the Born-Mayer repulsion contribution. $G_{|\vec{q}|}$ is composed of the wave-number-sum contribution to the electrostatic energy plus the energy wave-number characteristic:

$$\begin{aligned} A_{ii'}(\vec{r}) = & -(Z^2 e^2) \left\{ -\frac{\delta_{ii'}}{r^2} \left(\frac{2}{\sqrt{\pi}} \eta e^{-\eta^2 r^2} + \frac{\text{erfc}(\eta r)}{r} \right) \right. \\ & + \left[\frac{2}{\sqrt{\pi}} \eta e^{-\eta^2 r^2} \left(2\eta^2 r + \frac{3}{r} \right) + \frac{3}{r^2} \text{erfc}(\eta r) \right] \frac{r_i r_{i'}}{r^3} \Big\} \\ & - \alpha_r \gamma e^{-\gamma r} \left[-\frac{\delta_{ii'}}{r} + \left(\frac{\gamma}{r^2} + \frac{1}{r^3} \right) r_i r_{i'} \right], \end{aligned} \quad (14)$$

where α_r is the Born-Mayer repulsion coefficient and $1/\gamma = 0.339 \times 10^{-8}$ cm (Ref. 6),

$$G_{|\vec{q}|} = \frac{2\pi Z^2 e^2}{\Omega_a} \frac{e^{-q^2/4\eta^2}}{q^2} - \frac{\Omega_a q^2}{8\pi e^2} \frac{w_{B_q} w_{B_q} (f_q - 1)}{1 + (f_q - 1)(1 - g_q)}, \quad (15)$$

where w_{B_q} is the bare pseudopotential matrix element, f_q is the Hartree dielectric function, and $(1 - g_q)$ corresponds to an approximate correction due to exchange and correlation of the electron gas. For g_q we take

$$g_q = q^2/2 (q^2 + \xi k_F^2), \quad (16)$$

where k_F is the Fermi momentum and ξ is determined as in Ref. 4.

The other contributions to Eq. (12) are given by

$$\begin{aligned} v_{0ii'} = & \sum_{\vec{q}} G_{|\vec{k}+\vec{q}|} (\vec{k}+\vec{q})_i (\vec{k}+\vec{q})_{i'} \cos(\vec{Q} \cdot \vec{\delta}) \\ & + \sum_n A_{ii'}(\vec{r}_n + \vec{\delta}) \cos[\vec{k} \cdot (\vec{r}_n + \vec{\delta})], \end{aligned} \quad (17)$$

$$\begin{aligned} v_{1ii'} = & - \sum_{\vec{q}} G_{|\vec{k}+\vec{q}|} (\vec{k}+\vec{q})_i (\vec{k}+\vec{q})_{i'} \sin(\vec{Q} \cdot \vec{\delta}) \\ & + \sum_n A_{ii'}(\vec{r}_n + \vec{\delta}) \sin[\vec{k} \cdot (\vec{r}_n + \vec{\delta})]. \end{aligned} \quad (18)$$

The phonon-dispersion curves for hexagonal sodium are plotted in Fig. 3. The phonon frequencies and polarization vectors were calculated for 269

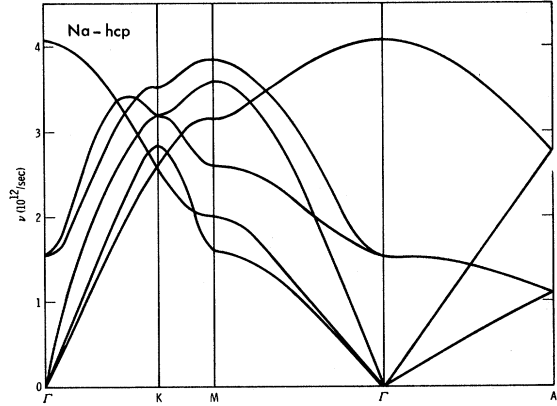


FIG. 3. Calculated phonon-dispersion curves for hcp sodium ($\nu = \omega/2\pi$).

points in $\frac{1}{24}$ of the first Brillouin zone.

The average phonon frequency squared is simply obtained from the average over \vec{k} of the trace of the dynamical matrices, and is given by

$$\begin{aligned} 3M\langle\omega^2\rangle = & \alpha_r \gamma \sum_n (\gamma - 2/r_n) e^{-\gamma r_n} \\ & + (4\pi Z e^2/3\Omega_a) + 2\sum_q' F_q q^2 (N^{-1} - S_q). \end{aligned} \quad (19)$$

The first term is the Born-Mayer repulsion contribution, the second term is the electrostatic-energy contribution, and the third term is the band-structure contribution. We may also obtain $M\langle\omega^2\rangle$ from Eq. (12) by first diagonalizing the dynamical matrix for each \vec{k} and performing the appropriate average over \vec{k} . A comparison of $M\langle\omega^2\rangle$ as calculated by Eqs. (12) and (19) provides a check on the accuracy of our lattice-dynamical calculations. Such a comparison showed a difference of less than 0.5% for both lattices. Equation (19) can give an approximate value for the average phonon frequency in the approximation of $M\langle\omega\rangle = M\langle\omega^2\rangle^{1/2}$. The results of such an approximation differ from the numerical solution and average over the Brillouin zone of $M\langle\omega\rangle$ as determined by Eq. (12) by about 7%.

The total free energy at $T=0$ consists of the static potential energy U_{static} plus the zero-point energy of the phonon modes. The zero-point energy was calculated from the average phonon frequency determined by averaging over the Brillouin zone. The addition of the zero-point energy changed the volume at which the free energy minimized, as is shown in Table I. The change in the values of the lattice constants with the inclusion of the zero-point energy was about the same for the bcc and hcp structures and worsened the agreement with experiment. The crystal-potential parameters, as discussed above, were determined in Ref. 4 with the

exclusion of the zero-point energy. Thus, the inclusion of this energy in the calculation of the lattice constants gives an increase in the lattice-constant values, as would be expected.

Knowing the phonon frequencies, we may now proceed to calculate the total temperature-dependent free energy as given in Eq. (9). The free energy must be calculated for each temperature of interest and then minimized with respect to the crystal configuration. The total free energy was calculated in the temperature range 0–280 °K. The free energy minimized at correspondingly larger volumes as the temperature increased, with a thermal expansion on the same order of magnitude as is observed experimentally. The thermal expansion could only be estimated since the different crystal configurations at which the free energy was calculated were not closely enough spaced to show thermal expansion for small temperature changes.

The total free energy as a function of temperature is plotted in Fig. 4. The crystal configurations used to plot this curve were those that gave the minimum free energy at each temperature. The bcc and hcp curves cross at $T = 260$ °K with the hcp free energy lower below 260 °K and the bcc free energy lower above 260 °K. The experimentally observed transition temperature is around 36 °K.

IV. DISCUSSION OF RESULTS AND CONCLUSION

We have calculated the total free energy as a function of temperature and the crystal configuration

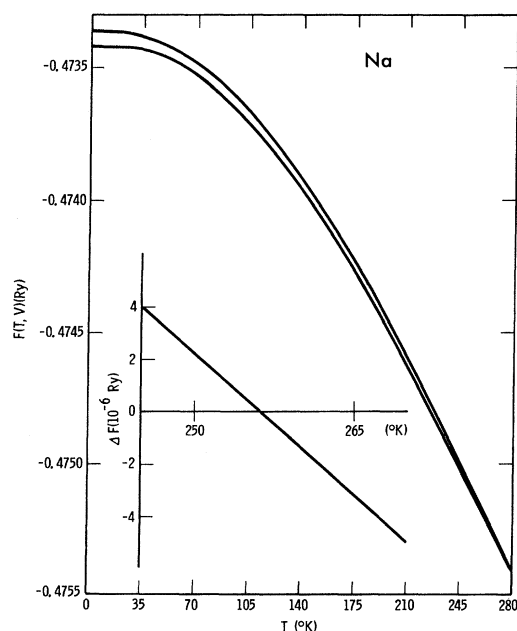


FIG. 4. Total free energy for hcp and bcc sodium. The insert plots the free-energy difference for the hcp and bcc structures.

by means of a local pseudopotential theory for the bcc and hcp phases of sodium. By minimizing the free energy at each temperature with respect to the crystal configuration, we are able to accurately determine the free energy at temperatures other than $T = 0$. At $T = 0$, we predict that the hexagonal structure is stable and remains stable until $T = 260$ °K, when the bcc structure becomes stable. The predicted transition temperature is higher than the observed temperature by a factor of 7. The inclusion of the zero-point energy at $T = 0$ causes the free energy to minimize at larger crystal volumes and gives poorer agreement with the experimentally determined lattice constants as indicated in Sec. III. However, since the resulting change in volume is about the same for both phases, the $T = 0$ energy difference between the two phases, which includes the zero-point energy, should not be appreciably affected, and indeed the value we calculate for the energy difference of the bcc and hcp phases is in closer agreement with experiment⁷ than previous calculations.^{2,3} Shaw's³ result shows an energy difference of 15×10^{-5} Ry and our difference is 6×10^{-5} Ry, while the experimentally determined value is 3.15×10^{-5} Ry. The improved experimental agreement that we obtain can be attributed to the minimization of the energy with respect to the crystal configuration and the inclusion of the zero-point energy, which decreases the energy difference since $\langle \omega \rangle_{\text{bcc}} < \langle \omega \rangle_{\text{hcp}}$.

The crystal potential as fitted by experimental data is known on an *a priori* basis to about 0.01 Ry, while the energy differences between the bcc and hcp phases of sodium are on the order of 5×10^{-5} Ry. One must consider whether such a pseudopotential model is accurate in calculating the small energy differences between the two structural phases. The pseudopotential-model parameters are determined by experimental data which has an accuracy of only 5% or better, and for the calculated energy difference to be of significance, one must consider the effect of the experimental uncertainty on the calculated energy differences. A change in the point-ion pseudopotential parameters of 3% produced a change in the structural-energy difference of 8% and a change in $\langle \omega^2 \rangle$ of 5%. A similar change in the Born-Mayer repulsion coefficients of 20% produced a change in the structural-energy difference of 10% and a change in $\langle \omega^2 \rangle$ of 2%. A change in the pseudopotential-model parameters corresponding to the 5% uncertainty in $\langle \omega^2 \rangle$ produces a maximum error of 25% in the calculated energy difference.

We have also calculated the energy differences between the bcc and hcp phases using different approximations for the exchange and correlation corrections for the electron gas, and using the tabulated values of Shaw's optimized-model potential for sodium.⁸ Using the interpolation functions of

Ref. 8 for the exchange and correlation corrections in the point-ion pseudopotential, the energy differences changed by 2%. The tabulated values of the form factors given in Ref. 8 also produced a similar change in the energy differences. This small change in the energy difference is below the accuracy of the pseudopotential and is not appreciably affected by the choice of the exchange and correlation corrections.

It is found that the thermal expansion of the crystal does not play a significant role in the phase transition. This is determined by calculating the total free energy as a function of temperature while keeping the crystal-configuration fixed. When the free energies of the bcc and hcp structures were compared in this manner, it was found that the free-energy curves cross again at approximately the same temperature as the full volume-dependent calculation.

The temperature effects arising from Fermi functions in the static potential have been ignored and are probably negligible since the temperatures of interest are much less than the Fermi temperatures of the alkali metals.⁹ Because of the relatively low Debye temperature, however, anharmonic effects will probably be important. Further, the anharmonic effects will be highly structure dependent since the selection rules governing the phonon-phonon interactions will be radically different for the bcc and hcp phases. With the inclusion of the anharmonic free energies, it is possible that the free energy of one of the two phases will be lowered relative to the other phase, yielding a lower transition temperature. The anharmonic free-energy calculations have not been carried out at the present time because of the difficulties associated with the hcp lattice with two atoms per unit cell.

At $T=0$, the hcp free energy is lower than that of the bcc structure. However, the average phonon frequencies are given by

$$\langle \nu \rangle_{\text{bcc}} = 2.50 \times 10^{12} \text{ sec}^{-1}; \quad \langle \nu \rangle_{\text{hcp}} = 2.55 \times 10^{12} \text{ sec}^{-1};$$

$$\langle \nu^2 \rangle_{\text{bcc}} = 7.16 \times 10^{24} \text{ sec}^{-2}; \quad \langle \nu^2 \rangle_{\text{hcp}} = 7.21 \times 10^{24} \text{ sec}^{-2}. \quad (20)$$

[The results given in Eq. (20) are for the crystal configurations that gave the minimum free energy at $T=0$.] Equation (20) shows that it is energetically easier, on the average, to excite a bcc phonon mode than an hcp phonon mode. This is primarily due to the existence of optic modes in the hcp structure which are absent in the bcc structure. As the temperature increases, the entropy for the bcc structure will increase more rapidly than for the hcp structure. The $T=0$ free-energy difference is finally overcome at $T=260^\circ\text{K}$ by the unequal increase in the entropy. The bcc structure continues to be more stable at higher temperatures.

The martensitic transformation actually occurring in nature is characterized by considerably hysteresis with some of the bcc phase transforming to a faulted hcp phase, and reversion to the bcc phase does not start until the sample is warmed to a temperature considerably above 36°K .¹⁰ The calculation that we performed was for perfect-crystal structures of the hcp and bcc lattice, while the transformation in nature certainly is not between perfect-crystal structures. The percentage of transformation to the hcp phase is likely to be highly dependent on the impurity content as well as the history of the sample. Barrett¹ observed that samples cold worked above the transition temperature could be induced to partially transform to the hcp phase, and it is likely that sodium partially forms a metastable faulted hcp phase above 36°K . However, the high calculated transition temperature may or may not reflect such a possibility because of the various approximations involved in pseudopotential theory.

ACKNOWLEDGMENT

The authors wish to thank Dr. N. S. Gillis for helpful comments.

[†]Work supported by the U.S. Atomic Energy Commission.

*Associated Western Universities Predoctoral Fellow, Colorado State University, Fort Collins, Colo.

¹C. S. Barrett, *Acta Cryst.* **9**, 371 (1956).

²W. A. Harrison, *Pseudopotentials in the Theory of Metals* (Benjamin, New York, 1966).

³R. W. Shaw, Jr., Ph. D. dissertation, Stanford University, 1968 (unpublished).

⁴D. C. Wallace, *Phys. Rev.* **176**, 832 (1968).

⁵(a) K. Fuchs, *Proc. Roy. Soc. (London)* **A151**, 585 (1935); (b) we have recently calculated α_{hcp} to much greater precision and find that α_{hcp} is not a maximum at ideal c/a , but the maximum occurs at $c/a=1.635639$

$\pm 3 \times 10^{-7}$ with $\alpha_{\text{hcp}}=1.791676902$. At $c/a=\sqrt{\frac{2}{3}}\alpha_{\text{hcp}}=1.691676241$.

⁶M. P. Tosi, in *Solid State Physics*, edited by F. Seitz and D. Turnbull (Academic, New York, 1964), Vol. XVI, p. 1.

⁷D. L. Martin, *Proc. Roy. Soc. (London)* **A254**, 433 (1960).

⁸R. W. Shaw, Jr., and R. Pynn, *J. Phys. C* **2**, 2071 (1969).

⁹W. J. L. Buyers and R. A. Cowley, *Phys. Rev.* **180**, 755 (1969).

¹⁰J. D. Filby and D. L. Martin, *Proc. Roy. Soc. (London)* **A276**, 187 (1963).